A cytoplasmic peptide of the neurotrophin receptor p75NTR: induction of apoptosis and NMR determined helical conformation

Matthew R. Hileman[a], Barbara S. Chapman[c], S. Rabizadeh[b], V.V. Krishnan[b], Dale Bredesen[b], Nuria Assa-Munt[b], Leigh A. Plesniak[a],*

[a]Department of Chemistry, University of San Diego, 5998 Acala Park, San Diego, CA 92110, USA
[b]Burnham Institute, La Jolla, CA 92037, USA
[c]Biological Sciences, California State University, San Marcos, San Marcos, CA 92096, USA

Abstract The neurotrophin receptor (NTR) and tumor necrosis factor receptor family of receptors regulate apoptotic cell death during development and in adult tissues [Beutler and van Huffel, Science 264 (1994) 667–668]. We have examined a fragment of p75NTR from the carboxyl terminus of the receptor and a variant form of this peptide via NMR techniques and in vitro assays for apoptotic activity. The wild type peptide induces apoptosis and adopts a helical conformation oriented parallel to the surface of lipid micelles, whereas the variant form adopts a non-helical conformation in the presence of lipid and shows no activity. These experiments suggest a link between structure and function of the two peptides.
© 1997 Federation of European Biochemical Societies.

Key words: Micelle; Spin label; Chemical shift index

1. Introduction

The neurotrophin receptor gp75NTR (NTR) is a member of a receptor superfamily that mediates cell survival, programmed cell death and cell differentiation in the immune and nervous systems [1]. Activation of NTR in the absence of a neurotrophin ligand induces programmed cell death in neurons and other cell types [2–4]. Increased expression of NTR has been associated with apoptosis in neurons [2] and increased sensitivity to the toxicity of β-amyloid peptide [4], a peptide which accumulates in the brains of patients of Alzheimer's disease [5]. Paradoxically, during embryonic development NGF binding appears to activate rather than block the death of function of NTR [6].

NTR, like TNFR (55 kDa), DR3, and DR4 and Fas, in-duces programmed cell death [7–10]. NTR has a sequence motif of 80–100 amino acid residues in its cytoplasmic tail which is homologous to 'death domains' found in Fas and TNFR-I [11]. In the case of Fas, DR3, DR4 and TNFR-1, signals resulting in programmed cell death (apoptosis) appear to be transmitted through protein-protein interactions involving this 'death domain' [9,10,12–14]. Activation of these receptors leads to recruitment of proteins involved in cell signaling to the plasma membrane [9,10,14]. The structure of the death domain of Fas has been recently reported [15].

Previous evaluation of structure-function relationships in the 'death domain' have concentrated on the residues having charged side chains (summarized in Huang et al. [15]). However, a potentially important hydrophobic surface is formed by helices five and six in the Fas death domain structure. The homologue of helix five in NTR is a peptide previously noted to contain homology to the wasp venom peptide mastoparan [11]. Mastoparan is a 14 residue peptide capable of activating heterotrimeric G-proteins, whose biological activity correlates with its ability to form an amphiphilic helix [16,17]. Furthermore mastoparan has been shown to induce apoptosis, both in whole cells [18] and in a cell-free system of apoptosis [19]. The homology of helix five to mastoparan suggested that an α-helical conformation within this region of the death domain of NTR may be a requirement for induction of apoptosis. To test the hypothesis that an α-helical segment forms part of an interface between NTR and the death signaling machinery, we have analyzed the structure of a 14 residue peptide from the human receptor using nuclear magnetic resonance (NMR), and a variant form of this peptide. We have also carried out in vitro assays for apoptotic activity in neuronal precursor cells on these peptides.

We have investigated the helix forming propensity of a peptide derived from NTR corresponding to residues 368–381 of the human receptor (NTR368) and a lysine variant of NTR368 (L373K). The choice of this analog (L373K) was based on the observation that a mastoparan variant having Lys instead of Leu at position 6 was both resistant to helix formation in 1-palmitoyl-1,2-oleoylphosphatidylcholine and unable to stimulate GDP/GTP exchange by Gαi protein [16]. NTR368 and mastoparan (Rabizadeh et al., submitted for publication) are potent inducers of neural apoptosis. We have also carried out in vitro assays which show that L373K does not induce neural apoptosis. The NMR studies demonstrate that NTR368 forms a helical structure in the presence of micellar lipid. These studies have also shown L373K does not have the ability to form a helical structure.

We have identified the optimal conditions for the NTR368 structure determination experiments and have found them to

be with a lipid:peptide of 9:1, consistent with conditions for dynorphin A [20]. Additionally, we have carried out NMR NOESY experiments at higher lipid concentration with a lipid:peptide of 50:1. These spectra were identical to the lower lipid concentration experiments; however, the line widths were broader. Thus, structural characterization was primarily carried out on the lower lipid concentration sample. We have carried out chemical shift indexing (CSI) which indicated that NTR368 has helical content. This is an ideal system for investigating the use of CSI with peptides bound to micelles, because we have a single amino acid mutation which does not adopt helical conformation as a control. Temperature coefficients were calculated that suggest solvent protection of one side of the helix. Finally, NMR studies using the nitroxide spin label, 12-doxyl stearate, show that the long helical axis of the peptide NTR368 is oriented parallel to the surface of the micelle and verify results suggested by the temperature coefficients.

Because of the difficulties involved with NMR structure determination in the presence of lipid, there are few published structures of peptides in the presence of micelles. Typically line widths are severely line broadened, $v_{1/2}$ approximately 15–20 Hz, making the determination of coupling constants impossible by homonuclear methods. The recently reported model of dynorphin A [21] and structure of magainin [22] are of superior quality and advance this area of structure determination. Most studies [23,24] have been carried out at higher lipid concentrations. Our studies have been carried out with a lower lipid concentration and have resulted in a comparable number of constraints, 6.8 inter-residue NOE constraints per amino acid.

These studies will lay the groundwork for investigations of the mechanism of induction of apoptosis in neurons, as well as, further characterization of the interactions between peptides and lipid interfaces.

2. Materials and methods

2.1. Peptide synthesis

A peptide was designed to represent the mastoparan homology found in residues 368–381 of human NTR [11]. This sequence is identical to rat NTR residues 365–378. The 14 residue sequence (ATLDALLAALRRIQ) was synthesized using standard scale Fmoc chemistry on an Applied Biosystems 430A automated synthesizer. The peptide (NTR368) was amino terminally acetylated and carboxy terminally amidated. A variant of this peptide (ATLDAKLAALRRIQ), representing a Lys substitution at residue 373 of human NTR, was also prepared. These peptides were cleaved from resin with trifluoroacetic acid in the presence of ethanedithiol and anisole, then purified by reversed phase HPLC on a Vydac semi-prep C_{18} column. Purity and molecular mass were verified by analytical HPLC and liquid secondary ion mass spectroscopy.

Two additional HPLC-purified peptides were purchased from Coast Scientific (San Diego, CA) for functional studies in tissue culture. A 26 residue peptide, containing the sequence of human NTR 367–380 (corresponding to rat NTR 364–377), was designed with 12 amino acid residues of the human immunodeficiency virus (HIV) *tat* protein, GRKKRRQRRRPP, at its amino terminus. The *tat* protein sequence improves the efficiency of peptide entry into cells [25]. The masses of *tat*-ATLDALLAALRRIQ (*tat*-NTR368) and a Lys substitution variant (*tat*-ATLDAKLAALRRIQ) called *tat*-NTR368-L373K were verified by mass spectroscopy.

2.2. Cell culture and peptide application

SH-SY-5Y (SH-SY) human neuroblastoma cells were grown and maintained in DMEM supplemented with 10% fetal bovine serum (FBS). For assays, SH-SY cells were plated onto 96-well plates. The

peptides *tat*-NTR368 and *tat*-NTR368-L373K were dissolved in water and diluted to 50 and 100 μM in serum free medium (SFM). Once diluted in SFM, the peptides were directly applied to the SH-SY cells in 96-well plates. After incubating for 18 h at 37°C, propidium iodide (20 μM) was added to the cells and cell viability was assessed in a Cytofluor fluorometric plate reader as described earlier [26].

2.3. NMR sample preparation

Three NMR samples were prepared. Two samples contained NTR368 at low and high lipid concentration. A third NMR sample was prepared containing a peptide identical to the NTR368 peptide except for a single amino acid substitution (L373K). The lipid used in these studies, dodecylphosphocholine-d_{38} (DODPC), purchased from Cambridge Isotope Laboratory (Andover, MA), was solubilized in H_2O to a concentration of 630 mg/ml by heating to 60°C and agitating with a vortex until clear and used as a stock solution for the addition of lipid to the NMR samples.

In the first sample, 8.0 mg of NTR368 was solubilized in 90 μl D_2O and 510 μl H_2O. A 1.0 M NaCl solution was used to make the sample 49 mM NaCl. DODPC and pH titrations were performed using a total of 30 μl of the DODPC stock solution and microliter amounts of 0.3 M NaOH and HCl, respectively. Conditions for optimal line widths and chemical shift dispersion for the low lipid concentration were found to be 7.7 mM NTR368, 69 mM DODPC, pH 5.2, and 49 mM NaCl.

In the second sample, 8.0 mg of NTR368 was solubilized in 70 μl D_2O and 600 μl H_2O. The 1.0 M NaCl stock solution was used to give a final NaCl concentration of 52 mM. Titrations of the lipid and pH were not performed on this sample, instead the pH was adjusted to 5.2, and 106 mg of DODPC was added to the sample. The concentrations of the second sample were 8.1 mM NTR368, 405 mM DODPC, pH 5.2, and 52 mM NaCl.

The third sample contained the lysine variant form of the NTR fragment, L373K. This sample was prepared by first dissolving 4.0 mg of the L373K peptide in 70 μl D_2O and 420 μl H_2O. The sample was then titrated with the stock DODPC solution in 10 μl increments to a total of 40 μl of the stock DODPC. A pH titration was also performed using the 0.3 M NaOH and HCl solutions. One-dimensional NMR spectra were used to examine the effects of the titrants. The conditions of optimal line widths and chemical shift dispersion were at pH 5.0, 4.9 mM L373K, and 118 mM DODPC. To confirm that the peptide was saturated with DODPC, more lipid was added beyond the concentration where chemical shifts remained constant and NMR experiments were repeated with similar results.

Finally, 3 μl of a 1.5 M stock solution of 12-doxyl stearic acid (purchased from Sigma) in *d*-chloroform was added to the NTR368 sample containing 405 mM DODPC. This yields a 60:1 ratio between DODPC:spin label.

2.4. NMR data collection

Proton NMR spectra were collected on Varian Unity 300 and Unity-plus 500 spectrometers operating at 300 and 500 MHz, respectively. The chemical shifts were measured relative to sodium 2,2-dimethyl-2-silapentane-5-sulfonate (DSS), used as an external reference. During data collection, the temperature was held at 25°C unless otherwise specified. All data were collected in the phase sensitive mode [27]. The spectra showed no contamination in the lipid as previously reported [20].

Two-dimensional DQF-COSY [28], TOCSY [29] and NOESY [30,31] experiments were carried out on the low lipid concentration sample at both 300 and 500 MHz. Water suppression was performed by use of presaturation coupled with a Hahn echo for narrowing of the H_2O resonance for the TOCSY and by the use of jump-and-return read pulse [32] for the NOESY. Water suppression was enhanced through zero frequency subtraction of the time domain [33]. The mixing times were 50 ms for the TOCSY and 150 ms for the NOESY. Two-dimensional NOESY spectra were also taken at 75, 100, and 125 ms in order to obtain a build up curve. This build up curve showed no spin-diffusion effects. There were a total of 512 measurements with 64 transients for each measurement taken at 500 MHz and a total of 600 measurements with 48 transients for each measurement taken at 300 MHz. At both 300 and 500 MHz, 4096 data points for t_2 were taken. Spectral widths for 300 and 500 MHz data collection were 4000 and 6000 Hz, respectively. Experiments with the spin label sample had sweep widths of 8000 Hz in the direct dimension and 6250 Hz in

the indirect dimension. The time-domain data were multiplied by gaussian multiplier functions in the direct dimension and a skewed squared sine bell function in the indirect dimension. For all data, the final processed matrices were 2048 by 2048 points in the frequency domain.

Two-dimensional TOCSY and NOESY experiments were run on both the high lipid concentration of NTR and the L373K peptide at 300 MHz, as described above at 25°C and 3°C. For both samples there were 4096 data points for t_2 taken, and spectral widths were both 4000 Hz.

2.5. Temperature coefficients and chemical shift indexing

TOCSY and NOESY spectra were collected on the low and high lipid concentration samples of NTR368 as described above at 3°C, 5°C, 16°C, 20°C, 25°C and 35°C. The amide proton chemical shifts were recorded and the temperature coefficients were calculated and recorded in parts per billion (ppb/°C). Chemical shift indexing was carried out as previously outlined [34]. The binary code, −1, 0 or +1 was recorded for α-proton chemical shifts. These experiments were also used as controls to verify exchange conditions of the peptide between free and micelle-bound forms.

2.6. Structure calculations

NOE constraint distances were assigned as previously described [35]. Structure calculations were carried out with the XPLOR 3.1 software package (Brünger, 1989) using the simulated annealing protocol [36,37]. Initial structures were generated with random coil geometry. Additionally, 11 initial structures were generated with unconstrained dynamics starting with unique random seed numbers. These structures were used to generate 90 annealed structures. Structures were subjected to a round of simulated annealing with backbone NOEs and then later again with side chain NOE constraints. These structures were minimized with a steepest descents and then conjugate gradient algorithm. The resulting structures were grouped into families and then evaluated for root mean square deviations (rmsd) and noe constraint violations.

3. Results

3.1. Biological effects of NTR368 and NTR368-L373K

The application of millimolar quantities of NTR367 to SH-SY medium resulted in cell death. Addition of the same concentrations of NTR367-L373K to SH-SY medium showed little or no effect on cell viability (data not shown). This suggested a relationship between the primary structure of
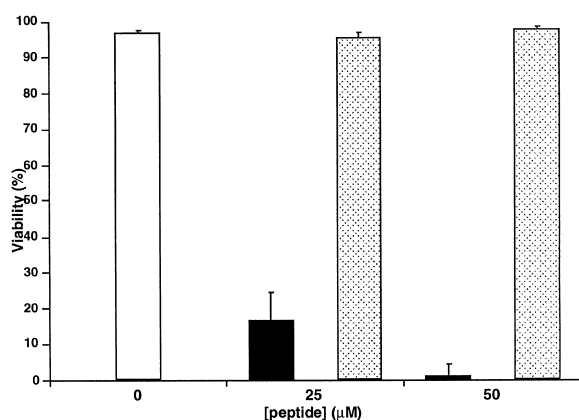

Fig. 1. Death induced by *tat*-NTR368 and not by *tat*-NTR368-L373K peptides in SH-SY cells. SH-SY cells were plated onto 96-well plates and were placed on SFM with either *tat*-NTR368 or *tat*-NTR368-L373K. Death was induced when SH-SY cells were placed in either 50 µM or 100 µM of *tat*-NTR368 (black) whereas the cells were unaffected by the *tat*-NTR368-L373K peptide (gray) as well as unsupplemented SFM (white). These data represent a single experiment in which each condition was applied and assessed in quadruplicates. Error bars represent standard deviations.

Table 1
Chemical shifts of NTR368

Residue	NH	α	β	γ	Other
A1		4.24	1.19		
T2	8.51	4.13	4.24	1.19	
L3	9.24	4.02	1.69	1.54	δ_1-0.97
					δ_2-1.00
D4	7.87	4.27	2.68		
A5	7.94	4.20	1.51		
L6	8.05	4.05	1.79	1.75	δ_1-0.83
					δ_2-0.87
L7	8.33	3.98	1.81	1.58	δ_1-0.90
					δ_2-0.84
A8	7.99	4.06	1.48		
A9	7.81	4.07	1.53		
L10	8.18	3.99	1.82	1.65	δ_1-0.82
					δ_2-0.84
R11	8.08	4.05	1.91	1.74	δ_1-3.18
					δ_2-3.13
					NH-7.36
R12	7.69	4.14	1.99	1.61	δ-3.22
					NH-7.50
I13	7.75	3.89	1.99	1.23	δ-0.84
				0.93	
Q14	7.85	4.07	2.05	2.31	
			2.10	2.42	

Proton chemical shifts (ppm) of 7.7 mM NTR in H_2O in the presence of 69 mM DODPC and 49 mM NaCl at pH 5.2 and 25°C.

the peptides and function. To insure that the biological effects of these two peptides were not the result of the NTR367 peptide's preferential ability to cross the cell membrane, a peptide from the HIV *tat* protein was attached to the peptide sequences. The *tat*-NTR368 fusion peptide affected toxicity in SH-SY cells. At concentrations exceeding 50 µM, *tat*-NTR368 induced greater than 97% cell death (Fig. 1). At the same concentration, *tat*-NTR368-L373K affected little toxicity relative to the absence of peptides. These results demonstrate that the difference in peptide effects is not due to a difference in membrane permeability and suggest that the region of the NTR corresponding to NTR368 may be involved in the receptor's ability to induce apoptosis. Moreover, the structural integrity of this region may determine its specificity for action and seems necessary to render its effects on neurons.

Having established that the two similar peptides had divergent biological activities, we looked to the three-dimensional structures for correlation. Because the peptides are small and flexible in solution, NMR structural studies were carried out in the presence of micellar lipid. The lipid provides a nucleation site for structure. We believe the function in the cell may be mediated either via protein:protein interactions or protein:lipid interactions.

3.2. NMR spectral assignment of resonances

Proton resonances of the low lipid concentration sample of NTR368 were identified by classical methods outlined by Wüthrich [38]. Spin systems were assigned by combination of DQF-COSY and TOCSY spectra (see Table 1). Sequential assignments were elucidated via comparison of TOCSY and NOESY spectra in the fingerprint region. Most helpful in the sequential assignments, were the intense dNN cross peaks. Spectra were acquired at 25°C and 35°C to resolve spectral overlap. Remaining ambiguities were resolved upon acquisition and analysis of the data at 500 MHz. The ^{1}H resonance assignments are listed in Table 1.
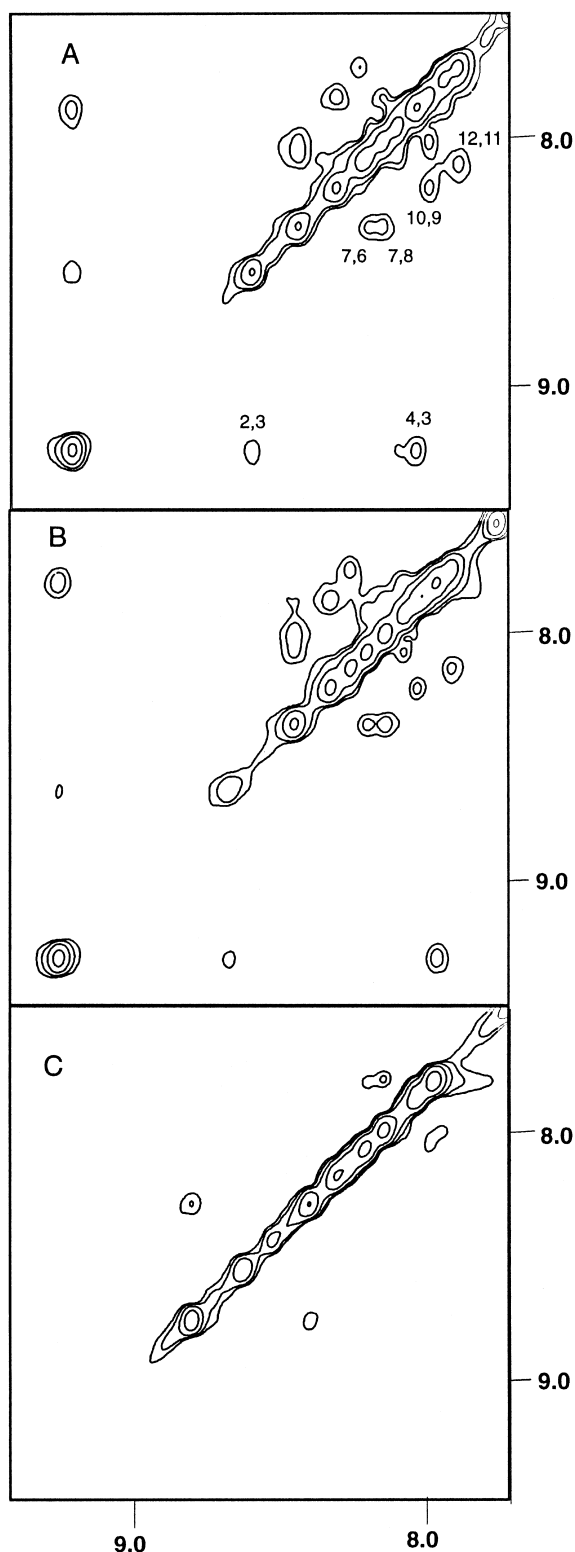
Fig. 2. Expansion of the amide section of a processed 150 ms mixing time 300 MHz NOESY acquired at 25°C. The spectra are from samples containing (A) 7.7 mM NTR368, 69 mM DODPC, 49 mM NaCl at pH 5.2, (B) 8.1 mM NTR368, 405 mM DODPC, 52 mM NaCl at pH 5.2 and (C) 4.9 mM L373K, 118 mM DODPC at pH 5.0. The spectra of NTR368 under conditions of high (B) and low (A) lipid concentrations are virtually identical. In contrast, these two spectra are markedly different from the NOESY of the peptide with a single leucine to lysine substitution in the sequence (C).

3.3. Comparison of high and low lipid concentration

The series of experiments carried out on the samples containing NTR368 clearly demonstrate that this peptide adopts a well-defined structure that is stable over a wide range of lipid concentrations (Figs. 2 and 3). Previous reports of peptide conformations have had substantially higher concentrations of DODPC [23,39] and other types of lipid [24,40], or have been carried out in fast exchange with vesicles [41]. Our studies indicate that the peptide adopts its structure at a lipid:peptide ratio of 9:1, and maintains this structure throughout the addition of DODPC to a lipid:peptide ratio of 50:1. This is in agreement with studies of peptides of this size previously reported [20]. The expansion of the amide region of NOESY spectra in Fig. 2, sections A and B, show that the peptide has the same chemical shifts and identical sequential connectivities under low and high lipid concentration. Inspection of Fig. 3 demonstrates that the fingerprint region and the amide, side chain regions of the NOESY spectra are virtually identical under these conditions as well. Minor differences in the spectra can be accounted for by the increase in line widths in the NTR368 sample containing 50:1 excess of DODPC. The line widths in the 50:1 lipid:peptide ratio sample and 9:1 lipid:peptide were 20 Hz and 15 Hz, respectively. Because of the narrower line widths, the lower concentration of lipid was used for data collection at 500 MHz and identification of NOE cross peaks. The quality of the data is illustrated in an expanded fingerprint region of a NOESY spectrum collected at 500 MHz field strength (Fig. 4).

3.4. Comparison of NTR368 and L373K spectra

In contrast to concentration of DODPC, a single amino acid substitution (L373K) in the NTR368 peptide has a profound influence on the peptide's structure in the presence of the micellar lipid. The 2D NOESY spectrum of L373K demonstrates that the peptide has either random coil or extended conformation. The absence of sequential dNN connectivities in the NMR NOESY experiments for the L373K peptide show that it does not form the same structure as the NTR368 peptide (Fig. 2C). CSI data also suggest that the peptide is random coil (Fig. 5). There is an absence of chemical shift dispersion which was observed in the other two NTR368 spectra (Fig. 2A,B), indicating that the L373K peptide adopts a non-helical conformation. NOE cross peaks in the amide, side chain region of the NOESY spectra suggest that the change in peptide binds to the micelle and adopts a non-helical structure. Without peptide association to the micelle, there would be *very* weak intensity NOE cross peaks because of the short correlation time of a peptide of this size.

3.5. Conformational analysis of NTR368

The secondary structural elements of the NTR368 peptide were elucidated primarily through analysis of the backbone NOEs. A summary of the backbone NOEs is shown in Fig. 6. A total of 103 NOEs were incorporated into structure calculations, including 23 $i,i+2$ NOEs and 32 NOEs between amino acids separated by three or more residues. The large line widths of the peptide prevent elucidation of dihedral angle constraints from DQF-COSY spectra.

The NOEs observed for this peptide were highly consistent with the conformation of an α-helix. There are 11 dNN cross peaks which are of medium intensity and 1 dNN cross peak with weak intensity. There are a total of six dNN (i,i+2) cross
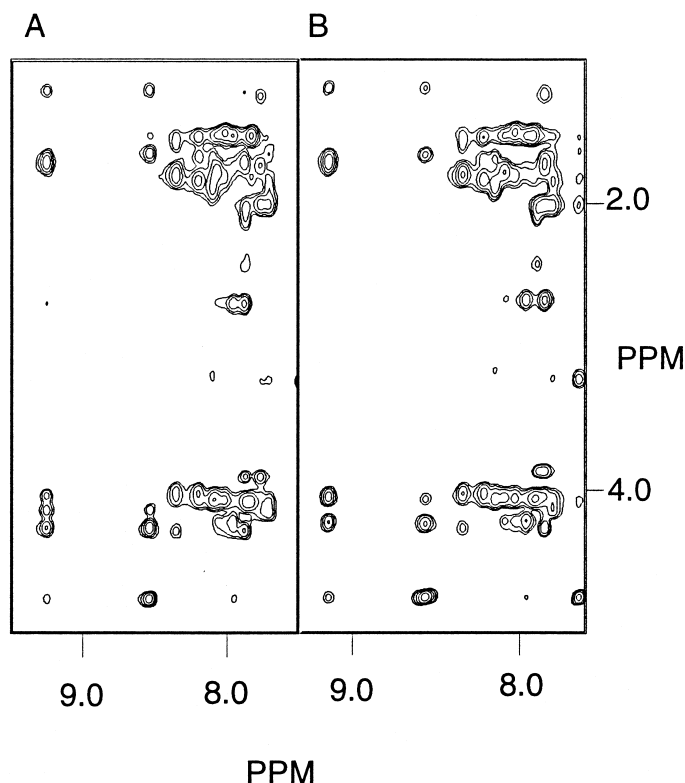
Fig. 3. Expansion of the amide, side chain section of 150 ms mixing time 300 MHz NOESY spectra from (A) a sample containing 7.7 mM NTR368, 69 mM DODPC, 49 mM NaCl at pH 5.2 and (B) 8.1 mM NTR368, 405 mM DODPC, 52 mM NaCl at pH 5.2. The spectra illustrate the extent to which the two sample conditions yield a peptide of identical conformation.

peaks which have been observed. Additionally there are two dNN (i,i+3) cross peaks observed at the amino terminal end of the peptide.

There are dαN NOE cross peaks which support that NTR368 adopts a helical structure. At the amino terminus there are four dαN (i,i+2) cross peaks and at the carboxyl terminus there are two dαN (i,i+2) cross peaks. The five dαN (i,i+3) cross peaks are distributed throughout the peptide; however, there are four dαN (i,i+4) cross peaks, all of which extend from the amino terminus.

The greater number of backbone helical NOEs at the amino terminus can be partially attributed to spectral overlap which prevents observation of these signals at the carboxyl terminus. This is illustrated by the presence of unfilled bars in Fig. 6 which denotes cross peaks which cannot be observed due to spectral overlap. However, the presence of the longest range dNN and dαN cross peaks exclusively at the amino terminus, suggests that the amino terminus of NTR368 forms a tighter helix than the carboxyl terminus which contains three consecutive bulky side chains, R11, R12 and I13.

The NOE constraints are generally equally distributed throughout NTR368. This is demonstrated in Fig. 5B which shows a graph of amino acid residue versus the number of NOE constraints which involve that amino acid. There are four alanines and four leucines in this 14 amino acid peptide. Chemical shift overlap in the side chains among the alanines and among the leucines provided the greatest hurdle in the structure determination.

The amino acids with the greatest number of NOEs generally have signals with the greatest chemical shift dispersion in the peptide. Asp[4] has the greatest number of constraints with

22 NOEs. Asp[4] has downfield shifted α and β proton resonances, which facilitate NOE elucidation. Thr[2], with 20 constraints, is another example of a residue with unique chemical shifts which enable elucidation of a greater number of NOEs. At 25°C, Arg[11] had many NOEs between its side chain and Ala[8], as well as Gln[14]. We suspected this was due to conformational exchange or perhaps spin diffusion effects. In NOESY experiments of the sample containing a low concentration of DODPC at 3°C, we found that the NOEs to Gln[14] were no longer present. We did not include the NOEs between Arg[11] and Gln[14] in the structure calculations. We believe that there was significant flexibility in the side chains which was reduced at 3°C.

Typical patterns of NOEs indicative of helical conformation are found throughout the peptide, but are concentrated near the amino terminus and the middle of the peptide. A large number of backbone *i,i+3* cross peaks are observed from
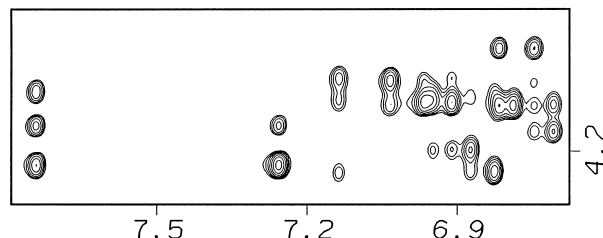

Fig. 4. This expansion of the fingerprint region of a 500 MHz NOESY spectrum collected at 25°C, 7.7 mM NTR368, 69 mM DODPC, 49 mM NaCl at pH 5.2 illustrates the quality of the data collected. With four leucines and four alanines in the peptide there is considerable overlap of signals in the α-proton dimension.

Asp[4]. Fig. 6B illustrates the central residues which show a large number of backbone *i,i+3* cross peaks, though there is not a wealth of total number of NOEs due to either short length of the side chains or spectral overlap.

3.6. Chemical shift indexing

The chemical shift of ^{1}H and ^{13}C signals is affected by their location in secondary structure. Thus, we have also analyzed the conformation of NTR368 with CSI of α-protons for further confirmation of the helical structure in NTR368 [34]. For comparison, we indexed the NTR368 as well as L373K, the lysine variant form which does not show propensity to form an α-helix in the presence of lipid. The CSI results in −1 for binary code for all amides in NTR368 with the exception of Ile[13]. The CSI for L373K was more randomly distributed, some 0 and −1 throughout the peptide. This supports our conclusion that NTR368 is helical and that L373K is not. It is also an example of CSI calculations on a small peptide in a lipid environment which is in agreement with NOESY data.

3.7. Temperature coefficients

Temperature coefficients were calculated from the slopes of chemical shift vs. temperature for the amide protons in NTR368. The calculations were carried out for both the low and high lipid concentration samples. The coefficients did not indicate the expected amide proton protection from solvent as a result of hydrogen bonding (Fig. 6). The temperature coefficients for the sample with low DODPC concentration are generally higher. This is expected because the sample with higher DODPC concentration will have a higher degree of
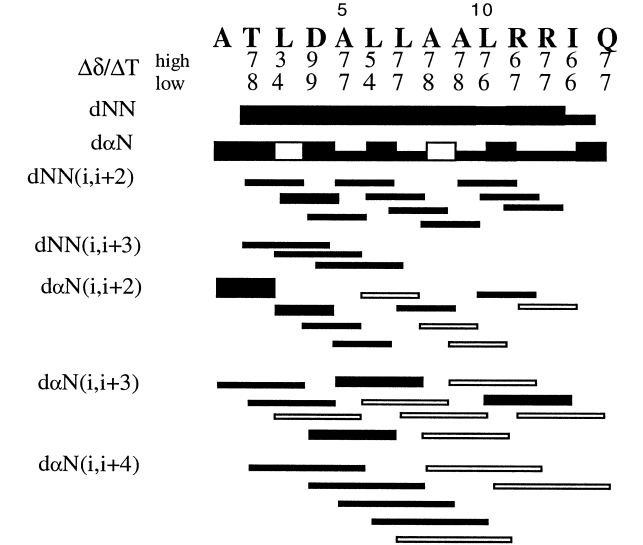

Fig. 6. NOE connectivities observed for 7.7 mM NTR in the presence of 69 mM DODPC and 50 mM NaCl, pH 5.2. The thickness of bars indicates strong, medium and weak NOEs with the thickest bars indicating strongest NOEs. Open bars indicate NOEs that *cannot* be observed due to spectral overlap. The top two rows of numbers are temperature coefficients in parts per billion for the two peptide samples containing high (8.1 mM NTR368, 405 mM DODPC, 52 mM NaCl at pH 5.2) and low (7.7 mM NTR368, 69 mM DODPC, 49 mM NaCl at pH 5.2) lipid concentrations.

peptide saturation of micelles. Interestingly, we noted lower temperature coefficients in both samples for Leu[3] and Leu[6] (Fig. 6). We note that Leu[10] on the low lipid sample and Arg[11] in the high lipid sample and Ile[13] have temperature coefficients lower than their neighboring amino acids. Independently, the structure calculations show that Leu[3], Leu[6], Leu[10] and Ile[13] are all on the same side of the α-helix. The fluctuations in the temperature coefficients suggest that the micelle is protecting one face of the α-helix from solvent exposure. We note that these residues are all strongly hydrophobic. The lower temperature coefficients clustered at the N-terminus of the helix is in agreement with NOE data and suggests that this terminus of the peptide forms a tighter helix. This may be a result of tighter association with the micelle interface, or an intrinsic property of the peptide.
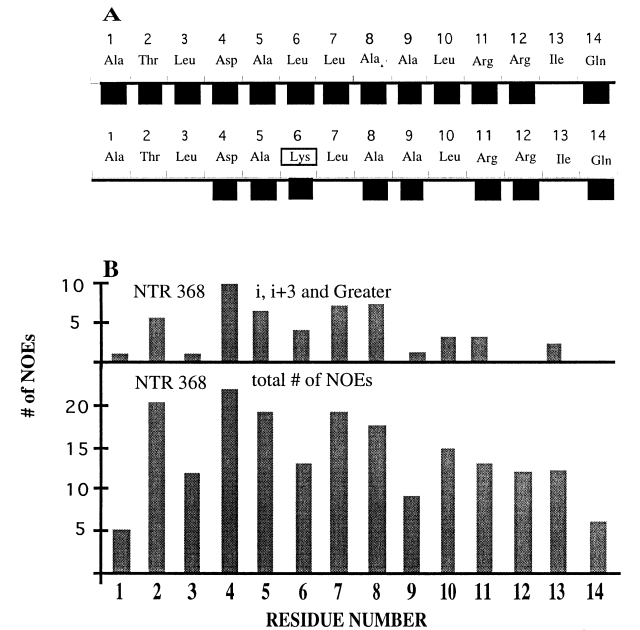

Fig. 5. A: The results of the CSI data for (top) NTR368, 7.7 mM NTR368, 69 mM DODPC, 49 mM NaCl at pH 5.2 and (bottom) for L373K, 4.9 mM L373K, 1118 mM DODPC at pH 5.0. The results indicate that NTR368 has chemical shifts for α-protons of an α-helical conformation while the α-proton signals of L373K sample exhibit random coil chemical shifts. B: A plot of the number of inter-residue NOE constraints per amino acid. This graph illustrates the extent and distribution of the NOE data. The top illustrates the distribution of *i,i+3* and *i,i+4* NOEs and (bottom) total number of NOEs. Note that each inter-residue NOE will appear two times in each section.

Table 2
Effect of spin label on NTR368

Residue	NH-αH	α
A1		23
T2	0	5
L3	0	0
D4	82	28
A5	10	23
L6	0	0
L7	0	–
A8	12	44
A9	0	22
L10	0	0
R11	7	31
R12	16	40
I13	6	16
Q14	100	18

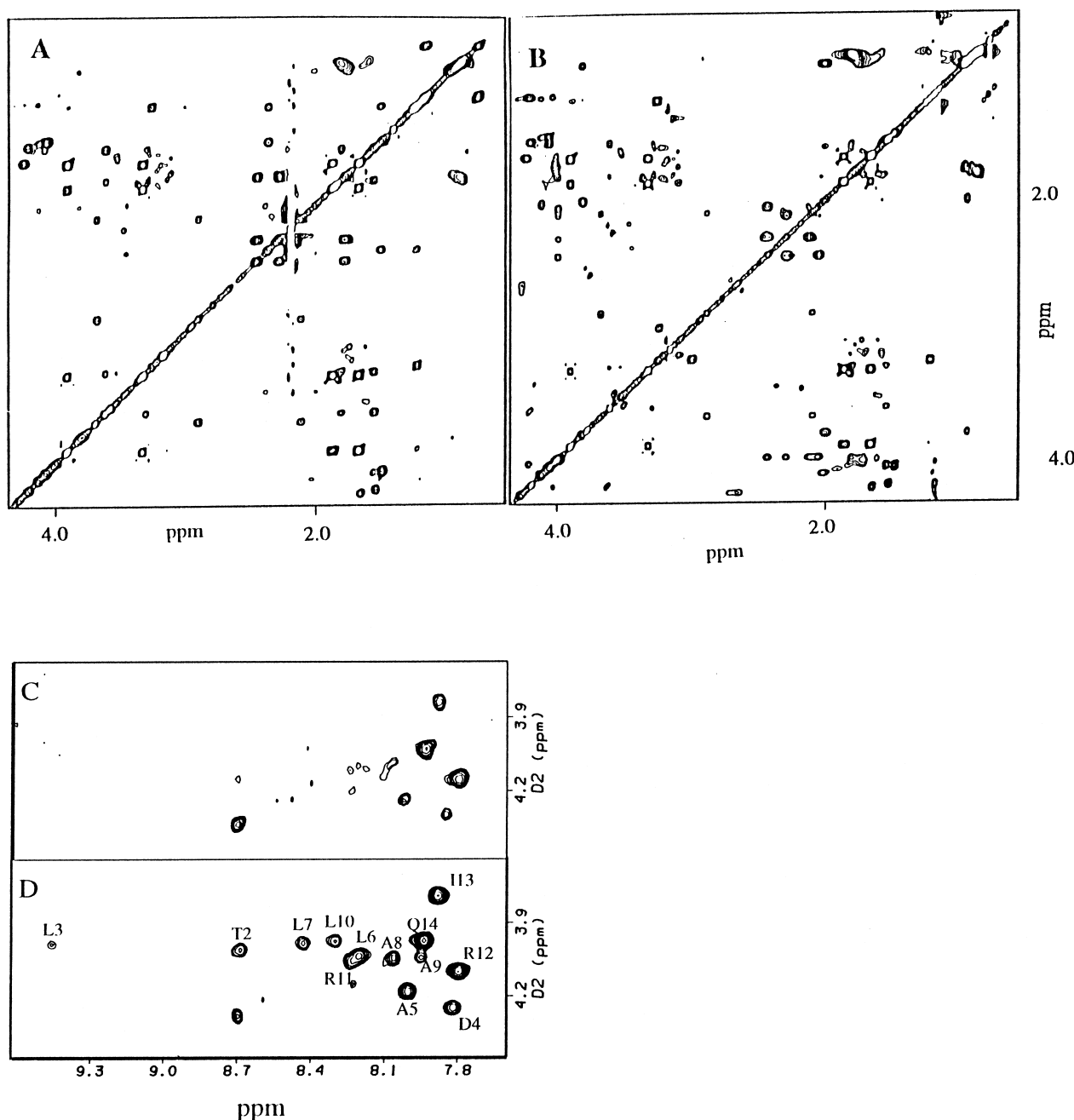% of ^{1}H NMR signal remaining in TOCSY spectra in the presence of 12-doxyl stearic acid.

Fig. 7. TOCSY experiments were carried out in the presence (A and C) and in the absence (B and D) of the spin label, 12-doxyl stearic acid. The experiments were carried out at 3°C, where conformational fluctuations in the carboxyl terminus of the peptide are at a minimum. The diminished signals indicate protons which are buried in the lipid environment of the DODPC micelle.

3.8. Experiments with 12-doxyl stearic acid

We were interested in further determination of the orientation of this peptide with respect to the surface of the micelle. We suspected it would be oriented parallel to the surface even though the sequence does not suggest this peptide is a true amphipathic helix. Towards this goal, 12-doxyl stearic acid (12-dox) was added to the NMR sample containing high concentration of DODPC. 12-dox carries an unpaired electron on the twelfth carbon of this fatty acid, thus positioning a free radical toward the center of the micelle. It has been shown previously (Brown, 1981 #5; Brown, 1982 #6) that 12-dox partitions into DODPC micelles and out of the aqueous environment. The unpaired electron provides an additional re-

laxation pathway for nearby protons and severely line broadens the NMR signals. In this case, signals of protons buried in the micelle will be diminished or eliminated upon addition of 12-dox.

As expected, the data show that the peptide is oriented parallel to the micelle surface with the leucines buried in the nonpolar environment. The results of the TOCSY experiment at 3°C (see Fig. 7A–D) summarized in Table 2 are in agreement with the temperature coefficient studies. Most signals were affected by the spin label, indicating a high degree of insertion of the peptide into the micelle. There are periodic fluctuations in the degree that ^{1}H signals were affected by the spin label, corresponding to the helical conformation of

NTR368. The fingerprint region signals (Fig. 7C,D) of Asp[4], Ala[5], Ala[8] and the carboxyl terminal residues Arg[11]–Gln[14] were least affected. These protons are in the aqueous environment. Similar trends were noted in the α,β proton cross peaks of the TOCSY. The NH, α cross peak of Gln[14] retained 100% of its previous intensity.

The leucine residues serve as a hydrophobic anchor of NTR368 as evidenced by the omission of all the four leucine signals in the fingerprint region and the α,β cross peak region (see Fig. 7A,B). These data also demonstrate an increase in surface exposure at the carboxyl end of the peptide. This is consistent with observations that the carboxyl end of the peptide exhibits mobility at room temperature.

3.9. Structure calculations

The results of structure calculations show the NTR368 peptide in helical conformation through the first 10 amino acids. The first round of simulated annealing calculations does not include side chain NOEs from Arg[11] and Arg[12]. The structures from these calculations result in helical conformation over the entire span of the peptide. These structures were then subjected to simulated annealing including the side chain NOE constraints from Arg[11] and Arg[12]. The result is an unwinding of the helix over the last four amino acids of the peptide.

The structure calculations yielded three families of structures, the largest family contained 17 structures. A superposition of this family is shown in Fig. 8D. The greatest consistent

Table 3
Agreement among NTR368 structures

Residue	Residues 1–14	Residues 1–10
A1	2.5	0.7
T2	1.5	0.3
L3	1.2	0.3
D4	1.0	0.3
A5	1.2	0.4
L6	1.2	0.5
L7	1.2	0.5
A8	1.7	0.6
A9	2.7	0.6
L10	1.4	1.8
R11	1.7	
R12	2.1	
I13	2.5	
Q14	3.7	

Rmsd (Å) of backbone atoms for 17 structures of family 1 of NTR368 based on alignments.

NOE violation (1.3 Å) is from Asp[4] βH to Leu[6] δH. The rmsd of the backbone atoms within this family of structures was 1.8 Å. A second alignment of the NTR368 structures was carried out over the first 10 residues of the peptide. With this alignment, the backbone rmsd of the first 10 residues was 0.6 Å. Finally, residues 11–14 were aligned to assess if there is a *hinge* in the peptide across which NOE data cannot link the structures. The rmsd of the last four amino acids of NTR368 is 1.32 Å. A summary of these alignments is shown in Table 3.

4. Discussion

Biochemical experiments have shown that addition of NTR368 to the media for neural cells induces apoptosis or cell death, while the addition of the same peptide with a single substitution, L373K, does not. The NMR studies demonstrate that NTR368 has helix forming propensity that is abolished by the single substitution in L373K, supporting one explanation for how this single amino acid substitution can have such a profound effect on the induction of the apoptotic pathway. Further studies to elucidate minimal components of this peptide for induction of apoptosis and corresponding NMR determinations of peptide conformation are being undertaken.

The helical structure of NTR368 in the presence of DODPC micelles spans from residues 1 to 10. These results support the model previously proposed [11] which predict the structure of NTR368 to be α-helical. After Leu[10], it is not clear to what extent the structure maintains an α-helical structure through the carboxyl terminus of the peptide. The absence of amide, amide long distance NOEs in this region of the peptide indicates a likely deviation from α-helical structure.

NTR368 is oriented parallel to the surface of the micelle, with a greater degree of peptide insertion in the middle residues (Ala[5]–Leu[10]). The residues of the helix which face the aqueous environment correspond to the amino acids Ala[1], Asp[4], Ala[8], Arg[12] and Gln[14]. NTR368 is not a true amphipathic helix, in that the entire middle of the peptide lacks a polar residue (sequence ALLAAL). NMR studies of peptide models of transmembrane spanning helices generally contain large numbers of alanines and leucines flanked by the positively charged amino acid, lysine. Such studies have been carried out with SDS as the lipid. SDS, which is negatively charged, has a favorable interaction with lysine while the alanines and leucines are inserted in the hydrophobic portion of
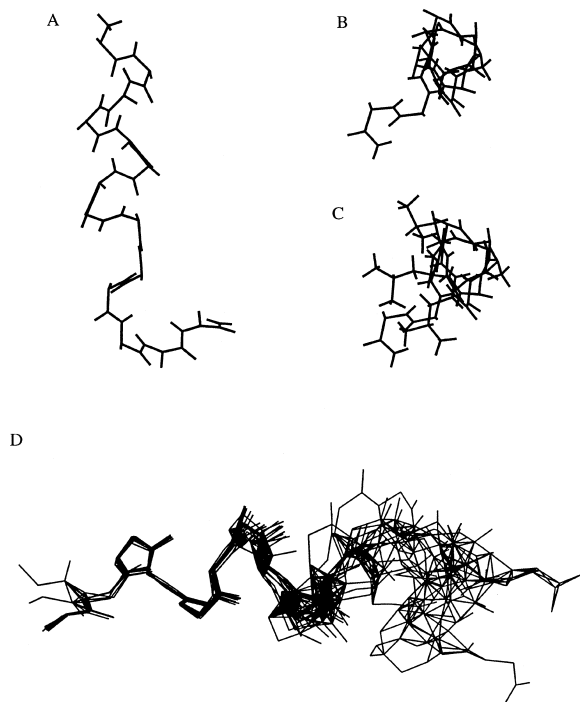

Fig. 8. The backbone atoms of a sample low energy structure of the NTR368 peptide, (A) shown from the side and (B) looking down the axis of the helix and (C) with the side chains of Leu[3], Leu[6] and Leu[10] shown. These are three amino acids with depressed temperature coefficients for their amide proton signals. Finally, (D) an overlay of 10 structures from a family of 17 structures. Three families of structures were calculated. This family contained the lowest number of NOE violations. The calculations were based on constraints from NOESY spectra in the presence of DODPC micelles; however, calculations are carried out in a vacuum without lipid present.

the micelles. NTR368 is insoluble in SDS and not long enough to allow the peptide to span a membrane or a DODPC micelle. Rather it interacts with the surface. We have identified the amino acids in the sequence which are most buried in the micellar lipid. These residues are Leu[3], Leu[6], Leu[7] and Leu[10]. Therefore peptide:lipid interactions are dominated by leucines.

Examination of the structures of the NTR368 peptide in the presence of DODPC micelles shows why L373K cannot form an amphipathic or membrane spanning-type α-helix. The position of lysine in L373K is on the side of the helix which contains entirely hydrophobic amino acids. Leu[3] and Leu[10] are also on this side of the helix, which face the micellar surface. Therefore, Leu[6] (now Lys[6]) is also in a position which the temperature coefficients and spin label data suggest to be facing the micelle surface. Both of these factors would contribute to disruption of the α-helix.

The quality of the structures has been hampered by the omission of hydrogen bonding constraints and dihedral angle constraints. We have attempted unsuccessfully to identify solvent protection of the amide hydrogens by measuring coupling constants and temperature coefficients. We have obtained NOE data 2D NOESY experiments from a variety of conditions. The next step for structure determination on a higher level of resolution is to isotopically label the peptide and carry out ^{1}H-^{15}N HMQC-J and NOESY 3D ^{15}N isotopically filtered experiments.

The sample conditions used for these experiments also illustrate that there is no *rule* for lipid:peptide ratios for NMR experiments. The optimal conditions for structural characterization of a peptide in the presence of micelles is dependent upon the individual system, peptide and type of lipid. We have noted that peptides larger than 20 amino acids or peptides which are inserted integrally into membranes require higher lipid concentrations [24] such that the micelle:peptide ratio is approximately 1:1. There are disadvantages to using higher lipid concentrations. The aggregation number of the micelles increases with lipid concentration [20], resulting in increased line widths.

The reporting of the structure of the Fas (APO-1/CD95) death domain has given us an opportunity to consider how this peptide functions to induce apoptosis. NTR368 corresponds to helix five of the NMR-determined structure of the Fas domain [15]. The homology between these regions of Fas and NTR [44] would place this peptide in helix five of the NTR death domain as well. Huang et al. [15] noted a hydrophobic patch on the surface of Fas was formed by helices five and six. Interestingly, a reported sequence alignment [11] shows that the corresponding hydrophobic patch in NTR would be even larger than that which is found in Fas. According to the sequence alignment by Chapman [11], two of the charged surface residues in Fas, Lys[272] and Asp[273], correspond to Ala[375] and Ala[376] of NTR. The Fas structure studies reported that alanine substitutions in the hydrophobic patch did not affect oligomerization of Fas or its interaction with FADD, its downstream signaling protein. These substitutions have focused on the electrostatic interactions via polar residues, lysine, aspartic acid and threonine. We postulate that function of the peptide, NTR368, requires the maintenance of the hydrophobic surface of this helix and that a disruption of this surface prevents NTR368 from interacting with the death machinery. The hydrophobic surface may serve to orient the

hydrophilic side of the helix toward death machinery or may interact with it directly.

Deber and coworkers have described systems with similar small perturbations in membrane environment or peptide sequence that can have large effects on structure of transmembrane spanning peptides and corresponding physiological effects [42,43]. Much work has been carried out investigating structure and function of the extracellular domains of the apoptotic receptors, but the current work examines a small fragment of the intracellular component of these receptors, sufficiently long to effect the apoptotic fate of neural cells. This work is of biological significance because of the demonstrated role of the neurotrophin receptor in neural cell death.

References

[1] Beutler, B. and van Huffel, C. (1994) Science 264, 667–668.
[2] Rabizadeh, S., Oh, J., Zhong, L., Yang, J., Bitler, C.M., Butcher, L.L. and Bredesen, D. (1993) Science 261, 345–348.
[3] Barrett, G.L. and Bartlett, P.F. (1994) Proc. Natl. Acad. Sci. USA 91, 6501–6505.
[4] Rabizadeh, S., Bitler, C.M., Butcher, L.L. and Bredesen, D.E. (1994) Proc. Natl. Acad. Sci. USA 91, 10703–10706.
[5] Glenner, G.G. and Wong, C.W. (1984) Biochem. Biophys. Res. Commun. 165, 166–167.
[6] Frade, J.M., Rodriguez-Tebar, A. and Barde, Y.A. (1996) Nature 383, 166–168.
[7] Frade, J.M., Rodriguez-Tebar, A. and Barde, Y.-A. (1996) Nature 383, 166–168.
[8] Casaccia-Bonnefil, P., Carter, B.D., Dobrowsky, R.T. and Chao, M.V. (1996) Nature 383, 716–719.
[9] Chinnaiyan, A.M. et al. (1996) Science 274, 990–992.
[10] Pan, G., O'Rourke, K., Chinnaiyan, A.M., Gentz, R., Ebner, R., Ni, J. and Dixit, V.M. (1997) Science 276, 111–113.
[11] Chapman, B.S. (1995) FEBS Lett. 374, 216–220.
[12] Boldin, M.P., Mett, I.L., Varfolomeev, E.E., Chumakov, I., Shemer-Avni, Y., Camonis, J.H. and D, W. (1995) J. Biol. Chem. 270, 387–391.
[13] Hsu, H., Xiong, J. and Goeddel, D.V. (1995) Cell 81, 495–501.
[14] Kischel, F.C., Hllbardt, S., Behrmann, I., Germer, M., Pawlita, M., Krammer, P.H. and Peter, M.E. (1995) EMBO J. 14, 5579–5588.
[15] Huang, B., Berstadt, M., Olejniczak, E.T., Meadows, R.P. and Fesik, S.W. (1996) Nature 384, 638–641.
[16] Higashijima, T., Burnier, J. and Ross, E.M. (1990) J. Biol. Chem. 265, 14176–14186.
[17] Danilenko, M., Worland, P., Carlson, B., Sausville, E.A. and Sharoni, Y. (1993) Biochem. Biophys. Res. Commun. 196, 1296–1302.
[18] Yan, G.M., Lin, S.Z., Irwin, R.P. and Paul, S.M. (1995) J. Neurochem. 65, 2425–2431.
[19] Ellerby, H.M., Martin, S.J., Ellerby, L.M., Naiem, S.S., Rabizadeh, S., Salvesen, G.S., Casiano, C.A., Cashman, N.R., Green, D.R. and Bredesen, D. (1997) J. Neurosci. (in press).
[20] Kallick, D.A., Tressmer, M.R., Watts, C.R. and Ching-Yuan, L. (1995) J. Magn. Reson. 109, 60–65.
[21] Tessmer, M.R. and Kallick, D.A. (1997) Biochemistry 36, 1971–1981.

[22] Gesell, J., Zasloff, M. and Opella, S.J. (1997) J. Biomol. NMR 9, 127–135.
[23] Inagaki, F., Shimada, I., Kawaguchi, K., Hirano, M., Terasawa, I., Ikura, T. and Go, N. (1989) Biochemistry 28, 5985–5991.
[24] McDonnell, P.A., Shon, K., Kim, Y. and Opella, S.J. (1993) J. Mol. Biol. 233, 447–463.
[25] Fawell, S., Seery, J., Daikh, Y., Moore, C., Chen, L.L., Pepinsky, B. and Barsoum, J. (1994) Proc. Natl. Acad. Sci. USA 91, 664–668.
[26] Kane, D.J., Ord, T., Anton, R. and Bredesen, D.E. (1995) J. Neurosci. Res. 40, 269–270.
[27] States, D.J., Haberkorn, R.A. and Ruben, D.J. (1982) J. Magn. Reson. 48, 286–292.
[28] Rance, M., Sørensen, O.W., Bodenhausen, G., Wagner, G., Ernst, R.R. and Wüthrich, K. (1983) Biochem. Biophys. Res. Commun. 117, 479–485.
[29] Bax, A. and Davies, D.G. (1985) J. Magn. Reson. 65, 355–360.
[30] Jeener, J., Meier, B.H., Bachman, P. and Ernst, R.R. (1979) J. Chem. Phys. 71, 4546–4553.
[31] Macura, S., Hyang, Y., Suter, D. and Ernst, R.R. (1981) J. Magn. Reson 43, 259–281.
[32] Plateau, P. and Guéron, M. (1982) J. Am. Chem. Soc. 104, 7310–7311.

[33] Marion, D., Ikura, M. and Bax, A. (1989) J. Magn. Reson. 84, 425–430.
[34] Wishart, D.S., Sykes, B.D. and Richards, F.M. (1992) Biochemistry 31, 1647–1651.
[35] Wüthrich, K., Billeter, M. and Braun, W. (1983) J. Mol. Biol. 169, 949–961.
[36] Nilges, M.G., Clore, G.M. and Gronenborn, A.M. (1988) FEBS Lett. 229, 317–324.
[37] Nilges, M.G., Clore, G.M. and Gronenborn, A.M. (1988) FEBS Lett. 239, 129–136.
[38] Wüthrich, K. (1986) John Wiley and Sons, New York.
[39] Brown, L.R. and Wüthrich, K. (1981) Biochim. Biophys. Acta 647, 95–111.
[40] Seigneruret, M. and Levy, D. (1995) J. Biomol. NMR 5, 345–352.
[41] Wakamatsu, K., Okada, A., Miyazawa, T., Ohya, M. and Higashijima, T. (1992) Biochemistry 31, 5654–5660.
[42] Li, S.-C., Kim, P.K. and Deber, C.M. (1995) Biopolymers 35, 667–675.
[43] Deber, C.M. and Li, S.-C. (1995) Biopolymers 37, 295–318.
[44] Chapman, B.S. and Kuntz, I.D. (1995) Protein Sci. 4, 1696–1707.